University of Dundee

Expression in Escherichia coli, purification and kinetic characterization of LAPLm, a Leishmania major M17-aminopeptidase

Aguado, Mirtha Elisa; González-Matos, Maikel; Izquierdo, Maikel; Quintana, Juan; Field, Mark C.; González-Bacerio, Jorge

Link to publication in Discovery Research Portal

Expression in *Escherichia coli*, purification and kinetic characterization of LAPLm, a *Leishmania major* M17-aminopeptidase

Mirtha Elisa Aguado[a,&], Maikel González-Matos[a,&], Maikel Izquierdo[a], Juan Quintana[b,†], Mark C. Field[b,c], Jorge González-Bacerio[a,*]

[a] Centro de Estudio de Proteínas, Facultad de Biología, Universidad de La Habana, calle 25 #455 entre I y J, Vedado, 10400 Havana, Cuba.

[b] Wellcome Centre for Anti-Infectives Research, School of Life Sciences, University of Dundee, Dow Street, DD1 5EH, Dundee, Scotland, UK.

[c] Institute of Parasitology, Czech Academy of Sciences, 37005 Ceske Budejovice, Czech Republic.

E-mail addresses: mirtha.aguado@fbio.uh.cu (MEA); maikel.gonzalez@fbio.uh.cu (MGM); mizquierdo@fbio.uh.cu (MI); juan.quintana@glasgow.ac.uk (JQ); mfield@mac.com (MCF); jogoba@fbio.uh.cu (JGB)

*Corresponding author. jogoba@fbio.uh.cu

[&]These authors contributed equally to this work

[†]Present address: Wellcome Centre for Integrative Parasitology (WCIP), Institute of Biodiversity, Animal Health and Comparative Medicine (IBAHCM), University of Glasgow, G61 1QH, Glasgow, Scotland, UK.

Running title: Expression, purification and characterization of LAPLm

ABSTRACT

The *Leishmania major* leucyl-aminopeptidase (LAPLm), a member of the M17 family of proteases, is a potential drug target for treatment of leishmaniasis. To better characterize enzyme properties, recombinant LAPLm (rLAPLm) was expressed in *Escherichia coli*. A LAPLm gene was designed, codon-optimized for expression in *E. coli*, synthesized and cloned into the pET-15b vector. Production of rLAPLm in *E. coli* Lemo21(DE3), induced for 4 h at 37ºC with 400 μM IPTG and 250 μM L-rhamnose, yielded insoluble enzyme with a low proportion of soluble and active protein, only detected by an anti-His antibody-based western-blot. rLAPLm was purified in a single step by immobilized metal ion affinity chromatography. rLAPLm was obtained with a

purity of ~10 % and a volumetric yield of 2.5 µg per liter, sufficient for further characterization. The aminopeptidase exhibits optimal activity at pH 7.0 and a substrate preference for Leu-p-nitroanilide (appK$_M$ = 30 µM, appk$_{cat}$ = 14.7 s^{-1}). Optimal temperature is 50ºC, and the enzyme is insensitive to 4 mM Co^{2+}, Mg^{2+}, Ca^{2+} and Ba^{2+}. However, rLAPLm was activated by Zn^{2+}, Mn^{2+} and Cd^{2+} but is insensitive towards the protease inhibitors PMSF, TLCK, E-64 and pepstatin A, being inhibited by EDTA and bestatin. Bestatin is a potent, non-competitive inhibitor of the enzyme with a K$_i$ value of 994 nM. We suggest that rLAPLm is a suitable target for inhibitor identification.

Keywords: expression in *E. coli*; IMAC; kinetic characterization; leucyl aminopeptidases; pET-15b vector

1. Introduction

Leishmaniasis is a disease caused by protozoan parasites of the genus *Leishmania*, transmitted by dipteran insects of the genera *Phlebotomus* and *Lutzomyia* [1]. *Leishmania* spp. cause a spectrum of diseases ranging from self-healing skin infection to progressive visceral illness, with the latter generally lethal [2]. The lifecycle is complex and involves two main hosts, the intermediate insect host and the vertebrate host. The infective metacyclic promastigote parasites, present in insect saliva, are transmitted by inoculation in the human blood. Promastigotes then invade different cell types, principally monocytes and macrophages, where they differentiate into amastigotes and replicate. Finally, the vector takes a promastigote-contaminated blood meal from an infected human and parasites replicate and differentiate onto metacyclic promastigotes. Leishmaniasis can be broadly classified into visceral, mucocutaneous and cutaneous leishmaniasis, depending upon the type of tissue colonized by the parasite [1]. Visceral leishmaniasis, mainly caused by *L. donovani* and *L. infantum*, affects the liver, spleen and bone marrow, causing progressive wasting, anemia and hepatosplenomegaly, with high mortality if untreated. Mucocutaneous and cutaneous leishmaniasis consist of skin and mucosal lesions of varying severity [1].

Leishmaniasis is prevalent in 88 countries, especially in Latin America but also Asia and Middle East, with 12 million people currently infected, 350 million at risk, ~1 million new cases reported and ~30,000 annual deaths [3]. No vaccine exists, and therapies are inadequate [4], highly toxic, difficult to implement and of limited

availability [5]. The most currently used chemotherapeutic agents against leishmaniasis include pentavalent antimony, amphotericin B and miltefosine [6]. Emerging resistance and reduced efficacy of available treatments accentuate the need for development of new drugs against novel targets [7].

Protozoan parasite proteases are increasingly relevant as virulence factors, drug targets and potential vaccine candidates, but few trypanosomatid peptidases have received attention, including a lysosomal cysteine peptidase [8], a cell surface metalopeptidase [9], a cytosolic serine oligopeptidase [10] and others. Metalo-aminopeptidases cleave the N-terminal residue from peptides and proteins [11] and are emerging as potential drug targets in parasites [12-17], but have been little studied in kinetoplastids, including *Leishmania* spp. The wide distribution of the metalo-aminopeptidases belonging to the M17 family (leucyl-aminopeptidases -LAP-; EC 3.4.11.1; [18]), and especially their essential roles in life cycles of various microorganisms [14,19-22], highlight the potential relevance of M17 LAP inhibitors for the treatment of these diseases and/or use in combined therapies.

Of *Leishmania* M17 LAP members, the basic LAP of *L. major* (LAPLm) has been studied and is a homohexameric protein of approximately 376 kDa, expressed by all parasite forms and responsible for the main LAP activity in *L. major* [13]. LAPLm appears to be involved in nutritional supply, since the parasite lacks the biosynthetic pathways for branched side chain amino acids, including leucine [23]. Consistent with this crucial role, arphamenine A, a *Trypanosoma cruzi* acidic M17 LAP inhibitor [24], inhibits *in vitro* growth of related *T. brucei brucei* [12], suggesting functional conservation across kinetoplastids. Down-regulation of TbLAP1, a *T. brucei* M17 LAP involved in mitochondrial kinetoplast DNA segregation during cell division, generates a cytokinesis delay [16]. Furthermore, the metalo-aminopeptidase inhibitor bestatin [25], causes *in situ* inhibition of the M17 LAP activity in *T. cruzi* epimastigotes [26], suggesting that endogenous LAPLm could be inhibited by bestatin-like low-molecular-weight inhibitors. Potent and selective LAPLm inhibitors could thus be starting points to develop antileishmanial drugs.

To search for LAPLm inhibitors, it is essential to have access to active enzyme, and other authors have successfully produced a version of recombinant LAPLm (rLAPLm) in *Escherichia coli* [13]. Considering the significance of LAPLm as a possible target for antileishmanial agents, rLAPLm was expressed in *E. coli*, after produce a synthetic gene

optimized for the bacterium, purified and kinetically characterized. This characterization indicated that rLAPLm has kinetic properties similar to other M17 LAPs. Therefore, this enzyme could be used as a target in a high-throughput screening assay.

2. Materials and Methods

2.1. Materials included in contracted services

The LAPLm (GeneBank code: **AF424693.1**) coding sequence, codon-optimized for expression in *E. coli* (Eurofins Genomics, Germany) was cloned into the *Nde*I/*Xho*I site of a pET-15b vector (Merck Millipore, Sweden).

2.2. Preliminary expression of the rlaplm gene in small-scale

The expression of the *rlaplm* gene was performed in the heterologous system *E. coli* Lemo21(DE3). First, to test the functionality of the genetic construction pET-15b-rLAPLm to sustain the *rlaplm* expression, a proof of concept was carried out at small-scale. A 5-mL-aliquot LB medium, supplemented with 100 μg/mL ampicillin and 30 μg/mL chloramphenicol, was inoculated with a colony of transforming cells and was incubated all night at 37ºC with shaking. Afterwards, 50 μl aliquots of this culture were removed and used as inoculums of 5-mL-aliquots of LB medium supplemented with ampicillin, chloramphenicol and different L-rhamnose concentrations (1, 20, 50, 100, 250, 500, 750, 1000 and 2000 μM). The rest of the former culture was kept at 4ºC for 3-4 days. The second cultures were incubated at 37ºC with shaking to reach an OD_{600nm} between 0.5 and 0.8, then induced with 400 μM IPTG and incubated overnight at 30ºC (for 1, 20 and 50 μM L-rhamnose) or for 4 h at 37ºC (for 100, 250, 500, 750, 1000 and 2000 μM L-rhamnose) under shaking.

As negative controls of expression were used a non-induced and an induced culture of the strain transformed with the pET-15b-rLAPLm construction, both in ampicillin and chloramphenicol-supplemented LB medium without L-rhamnose. The expression of *rlaplm* was assessed by polyacrylamide gel electrophoresis in denaturing conditions (SDS-PAGE with NuPAGE 4-12 % Bis-Tris Gels and Coomasie Blue R-250 staining; [27]), western-blot with an anti-His antibody, and enzymatic activity (EA) determination using the chromogenic substrate Leu-*p*-nitroanilide (Leu-*p*NA) (Bachem,

Sweden). Densitometric analysis of the gel images were performed with the software ImageJ (version 1.38d; National Institutes of Health, USA [http://rsb.info.nih.gov/ij/]). An 850-µL-aliquot, from the culture conserved at 4ºC, was mixed with 150 µL of sterile glycerol. The cells were divided in 100-µL-aliquots and flash frozen for the conservation of the positive clone at -70ºC.

2.3. Expression of the rlaplm gene in 300-mL-scale

Five-mL-aliquots of ampicillin and chloramphenicol-supplemented LB medium were inoculated from cryo stocks of the rLAPLm producing bacterial clone and incubated overnight at 37ºC with shaking. Three-mL-aliquots of these cultures were used to inoculate four 300-mL-aliquots of LB medium supplemented with ampicillin, chloramphenicol and 250 µM L-rhamnose. The 300 mL cultures were incubated at 37ºC with orbital shaking at 125 rpm until they reached an OD_{600nm} between 0.5 and 0.8, then induced with 400 µM IPTG and incubated overnight at 30ºC with shaking.

OD_{600nm} was measured and bacterial biomass was collected by centrifugation at $8,000 \times g$ for 15 min at 4ºC (Centrifuge 5810R, 15 amp version, Eppendorf AG, Germany). The bacteria were resuspended in cold 50 mM Tris-HCl buffer pH 8.0, 300 mM NaCl, until a cell suspension with a concentration of 10 units of OD_{600nm} was achieved. The cells were broken by sonication for 6 min (2 min pulse, 40 % output, 2 min pause over ice) (Soniprep 150 MSF, England) and cell debris separated by centrifugation at $12,000 \times g$ for 30 min at 4ºC. The supernatants were stored at -20ºC. Protein concentration was assessed in the supernatants by the bicinchoninic acid method [28].

2.4. Western-blot

rLAPLm is expressed with a N-terminal His-tag, to help in the purification by immobilized metal ion affinity chromatography (IMAC). This allowed performing a western-blot with an anti-His antibody to detect the protein in the bacterial soluble extract. For this, proteins were transferred from SDS-PAGE gel to PVDF iBlot2 Mini Stacks membranes (Invitrogen) in an iBlot2 (Invitrogen) 2 Gel Transfer Device equipment (Israel) for 6 min. Afterward, it was blocked for 1 h with 5 % milk in TBS (1 L: 100 mL 5 M NaCl, 20 mL 1 M Tris pH 7.5, 1 mL 0.1 % Tween 20). A mouse anti-His antibody (1:3000; Thermo Scientific/Pierce Biotechnology, USA) was applied for 1 h, it was washed for 1 h with TBS (five changes), and a peroxidase-conjugated anti-mouse secondary antibody (1:10000; Thermo Scientific/Pierce Biotechnology, USA)

was applied overnight at 4ºC. Finally, it was washed for 1 h with TBS (five changes) and developed with ECL (luminol, H_2O_2, cumaric acid).

2.5. Purification of the rLAPLm enzyme by IMAC

Purification of the rLAPLm enzyme was performed by IMAC from *E. coli* Lemo21(DE3) soluble extracts enriched in the recombinant enzyme, using a 5-mL-column packed with a HisPur™Cobalt matrix (Thermo Scientific/Pierce Biotechnology, USA) in Akta Prime. The matrix was equilibrated with five column volumes (CV) of cold binding buffer (50 mM Tris-HCl pH 8.0, 300 mM NaCl). After loading 100 mL of the protein extract, the column was washed with the same buffer until the absorbance at 280 nm descended until the base-line. Afterward, it was washed with five CV of cold washing buffer [50 mM Tris-HCl pH 8.0, 300 mM NaCl, 20 mM imidazole (Sigma, USA)]. Finally, the protein was eluted with a linear gradient of cold elution buffer (50 mM Tris-HCl pH 8.0, 300 mM NaCl, 20-400 mM imidazole). Two mL fractions were collected. Runs were monitored by checking the absorbance at 280 nm, using as blank the corresponding buffer of each step to eliminate the contribution of the imidazole to the absorbance.

The obtained fractions were evaluated by SDS-PAGE. The eluates were desalted by gel filtration chromatography, using a NAP-10 column (Sephadex G-25 Medium; Sigma, USA) to eliminate the imidazole. Afterward, the aminopeptidase EA was assessed toward the Leu-*p*NA substrate.

2.6. Determination of rLAPLm aminopeptidase enzymatic activity

The aminopeptidase EA was determined by a continuous kinetic method [29]. The chromogenic Leu-*p*NA substrate was used at 300 µM (2 µL added from a 30 mM stock dissolved in DMSO) and the increasing of OD_{405nm}, due to *p*-nitroaniline chromogen liberation, was recorded over 5 min using a spectrophotometer (FLUOstar OPTIMA, Germany). The determinations were carried out at 50ºC in 96-well plates in a reaction volume of 200 µL. EA buffer (50 mM sodium phosphate pH 7.0, 4 mM $MnCl_2$) was used, and volumes of protein extract or concentrations of the purified enzyme (1.39 × 10^{-8} M) were chosen in the range of a linear relationship among these magnitudes and the enzymatic reaction initial velocity (v_0). DMSO was ≤ 2 % of the final volume of the reaction mixture. Only the linear ranges of the typical curves, corresponding to substrate consumptions lower than 5 % (v_0 conditions) were used to measure the reaction

velocity. Slopes with determination coefficients (R^2) < 0.98 were not considered for linear fits.

The EA unit (U) is defined as the amount of enzyme necessary to hydrolyze 1 μmol substrate per minute under assay conditions. The used molar extinction coefficient at 405 nm for *p*NA was 9.87 mL/μmol/cm [30]. The EA in U/mL is defined as the ability of 1 mL enzymatic solution to hydrolyze 1 μmol substrate per minute in the assay conditions. The specific EA (specEA), expressed in U/mg, is calculated as the ratio between EA in U/mL and protein concentration in mg/mL. The assays were carried out in v_0 conditions in quadruplicate and the results presented as the mean ± the standard deviation.

2.7. Inhibition assay of rLAPLm aminopeptidase activity by bestatin

Twenty μL of the protein extract were mixed with EA buffer supplemented with 80 μM bestatin (Bachem, Sweden; 2 μL added from a 8 mM stock dissolved in DMSO) and this mixture was preincubated for 30 min at 25ºC and pH 7.0 before adding the Leu-*p*NA substrate at 30 μM (~1 apparent K_M -appK_M-). All other experimental conditions were maintained as described above. The control was prepared by extract and buffer preincubation omitting bestatin (with 2 μL DMSO). Residual activity (v_i/v_0) was defined as the quotient between the reaction velocity in the presence of bestatin and the control.

For the dose-response study, different bestatin concentrations were used (prepared in DMSO by double serial dilutions) spanning the range 0.781-100 μM (assay concentrations). The medium inhibitory concentration (IC_{50}) value was calculated by the non-linear fit of the logistic function to the experimental data, using OriginPro 8 SR0 software (version 8.0724 (B724); OriginLab Corporation [http://www.OriginLab.com]) with default parameters. The logistic function is: $y = 1/(1 + [I]/ IC_{50})$, where y: residual aminopeptidase activity, and [I]: inhibitor concentration in the assay [31]. All assays were performed by quadruplicate.

For the determination of the inhibition mode, bestatin was used at 0, 5 and 10 μM. For each inhibitor concentration, the substrate Leu-*p*NA was added at different concentrations, spanning the range 18.75-300 μM in the assay. The experimental data were transformed and the Lineweaver-Burk double reciprocal plots were constructed. The equation is: $1/v_0 = (appK_M/appv_{max}) (1/[S]_0) + 1/appv_{max}$, where $appv_{max}$: apparent

maximal rate of the enzymatic reaction, and $[S]_0$: initial substrate concentration in the assay [31]. The inhibition type was determined graphically from the lines of the double reciprocal plots [31]. K_i was determined by Dixon plot ($1/\text{app}v_{max}$ *vs.* [I]), to determine the -αK_i value, and the other secondary plot (slope Lineweaver-Burk plots *vs.* [I]), to determine the -K_i value [31]. The transformed experimental data were analyzed by a simple linear fitting using the software Microsoft Office Excel 2007™ (Microsoft Corporation; USA; [https://www.microsoft.com/]).

2.8. pH dependence of rLAPLm aminopeptidase activity

The pH effect over the aminopeptidase activity of the rLAPLm enzyme was assessed in the pH range 4.0-12.0 using different buffers (100 mM sodium acetate + acetic acid for pH 4.0 and 5.0, 100 mM PBS for pH 6.0 and 7.0, 50 mM Tris-HCl for pH 8.0-10.0, 1 M glycine + NaOH for pH 11.0 and 12.0) and 300 μM Leu-*p*NA substrate (assay concentration; ~10 appK_M). All other experimental conditions were maintained as described above. Relative activity was defined as the quotient between the reaction velocity at a value of pH and the maximal velocity measured among all pH values analyzed (expressed as percentage). Means were compared by the Tukey HSD test [32] using a signification level of 0.05 and the software STATISTICA v8.0.550.

2.9. rLAPLm aminopeptidase substrate specificity

The aminopeptidase EA of purified rLAPLm was tested in the presence of 300 μM of different *p*NA chromogenic substrates: Leu-, Arg-, Ala-, Gly-, Val-, Pro-, Lys-, Ile- and Glu-*p*NA (Bachem, Sweden). Relative activity was defined as the quotient between the reaction velocity toward a substrate and the maximal speed measured among all substrates tested (expressed as percentage). Means were compared by the Tukey HSD test [32] using a signification level of 0.05 and the software STATISTICA v8.0.550.

2.10. Determination of the kinetic parameters of the rLAPLm enzyme

For the determination of the kinetic parameters of the rLAPLm enzyme, aminopeptidase activity assays were performed at six concentrations of the Leu-*p*NA substrate, prepared by double serial dilutions covering the range: 9.375-1200 μM (assay concentrations). All other experimental conditions were maintained as described above. The kinetic parameters: appK_M and apparent catalytic constant (appk_{cat} = $v_{max}/[E]_0$, where $[E]_0$: initial free enzyme concentration in the assay) were calculated by fitting the function of the Michaelis-Menten's rectangular hyperbola to the experimental data [31]. Data

analysis and curve fitting were performed with the software OriginPro 8 SR0 (version 8.0724 (B724); OriginLab Corporation [http://www.OriginLab.com]).

2.11. Study of the effect of temperature on rLAPLm aminopeptidase activity

For the determination of the optimum temperature of purified rLAPLm aminopeptidase EA, the reaction was performed at different temperatures (20, 25, 30, 37, 40, 50, 60, 70, 80 or 90ºC) in the presence of 300 μM Leu-pNA substrate (assay concentration; ~10 appK_M). All other experimental conditions were maintained as described above. Relative activity was defined as the quotient between the reaction velocity at one given temperature and the maximal velocity measured among all assessed temperatures (expressed as percentage). Means were compared by the Tukey HSD test [32] using a signification level of 0.05 and the software STATISTICA v8.0.550.

2.12. Study of the effect of different divalent cations on rLAPLm aminopeptidase activity

For the determination of the effect of different divalent cations on purified rLAPLm aminopeptidase EA, the reaction was performed in the presence of different divalent cations ($CoCl_2$, $MnCl_2$, $MgCl_2$, $CdCl_2$, $BaCl_2$, $CaCl_2$ or $ZnCl_2$; Sigma, USA) at a concentration of 4 mM and 30 μM Leu-pNA substrate (assay concentration; ~1 appK_M). All other experimental conditions were maintained as described above. Residual activity was defined as the quotient between the reaction velocity in the presence of a given metallic cation and the reaction velocity of the control without divalent cation addition (expressed in times). Means were compared by the Dunnett test [33] using a signification level of 0.05 and the software STATISTICA v8.0.550. There were negative controls omitting the enzyme to rule out catalytic activity of divalent cations.

2.13. Determination of the inhibition profile for rLAPLm aminopeptidase activity toward inhibitors of different mechanistic classes

The inhibition profile for the rLAPLm enzyme was determined with the following protease inhibitors: 100 μM bestatin (inhibitor of different metalo-aminopeptidases; [34]), 10 mM EDTA (metalo-protease inhibitor), 2 mM PMSF (serine-protease inhibitor), 10 μM TLCK (serine-protease inhibitor), 10 μM E-64 (cysteine-protease inhibitor), and 200 μM pepstatin A (aspartyl-proteases inhibitor) (Sigma, USA) [35]. All indicated inhibitor concentrations are the final assay concentrations and 2 μL were added from a 100× stock. The enzyme-inhibitor mixtures were preincubated for 30 min at 25ºC and pH 7.0 before adding the Leu-pNA substrate at 30 μM (~1 appK_M). All

other experimental conditions were maintained as described above. Controls were prepared by preincubation of the enzyme with the same volume of the solvent used to dissolve the respective inhibitor, under the conditions mentioned above. Residual activity was defined as the quotient between the reaction velocity in the presence of the inhibitor and the reaction velocity of the control (expressed as percentage). Means were compared by the Dunnett test [33] using a signification level of 0.05 and the software STATISTICA v8.0.550.

3. Results

3.1. pET-15b-rLAPLm genetic construction optimized for the rlaplm gene expression in Escherichia coli

To facilitate production of rLAPLm (GeneBank code: **AF424693.1**) in *E. coli*, we designed a 1710 bp synthetic fragment for expression of soluble protein with an approximate molecular mass of 62 kDa (Fig. 1). The 1695 bp coding sequence was codon optimized and fused to an *Nde*I restriction site at the 5' end and two stop codons followed by an *Xho*I restriction site at the 3' end.
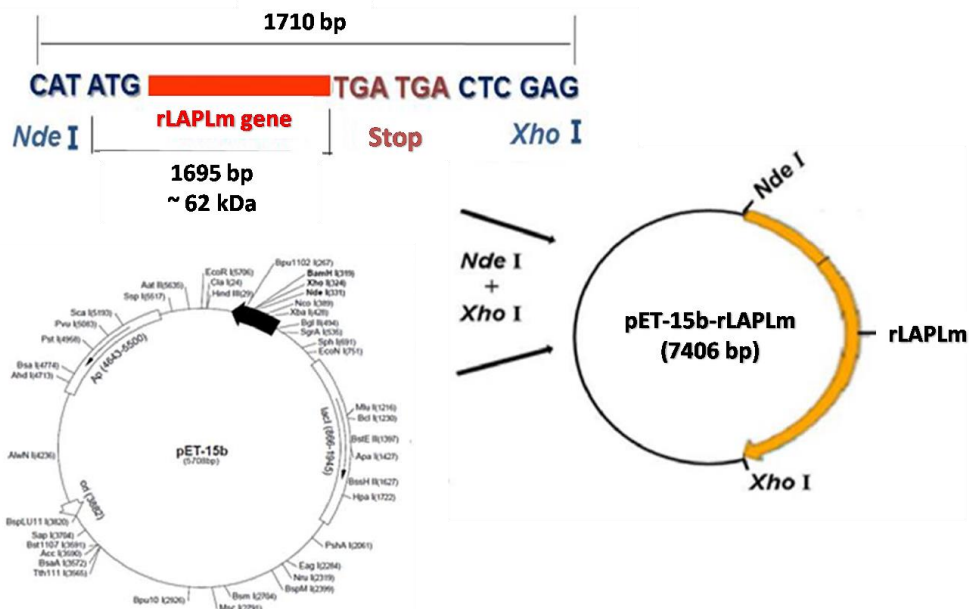

Fig. 1. Cloning of the *rlaplm* gene in the vector pET-15b. The synthetic gene, the pET-15b *Escherichia coli* expression vector and the resulting pET-15b-rLAPLm plasmid are shown. In the schematic plasmid map, the rLAPLm gene and the location of the *Nde*I and *Xho*I restriction sites are represented. Other genetic elements, as the T7*lac*

promoter, the *lac*O operator, the *lac*I gene, the pBR322 replication origin and the ampicillin resistance gene, were omitted for clarity.

The *rlaplm* gene sequence was optimized and synthesized (Eurofins Genomics, Germany) showing a codon adaptation index in *E. coli* of 0.79. The synthetic *rlaplm* gene was cloned into the *E. coli* expression plasmid vector pET-15b using the *Nde*I and *Xho*I restriction sites, placing transcription under the control of the strong and inducible T7*lac* promoter. The resulting plasmid of 7406 bp was termed pET-15b-rLAPLm (Fig. 1). The plasmid encodes rLAPLm fused to an N-terminal tag of six histidines and a 10 amino acid linker (sequence: SSGLVPRGSH).

3.2. Expression of the rlaplm gene in the heterologous system Escherichia coli Lemo21(DE3)

E. coli Lemo21(DE3) competent cells were transformed with the pET-15b-rLAPLm plasmid and one clone was selected to confirm expression of the recombinant protein. This strain contains an additional plasmid codifying lysozyme (inducible by L-rhamnose), a T7 RNA polymerase inhibitor. In this manner, in the presence of L-rhamnose lysozyme is induced, which inhibits the T7 RNA polymerase and decreases the expression rate of LAPLm in the presence of IPTG, potentially allowing for a better and more controlled folding conditions, leading to higher yields of soluble protein. This preliminary expression experiment was performed in 5 mL of LB medium.

First, different L-rhamnose concentrations (100-2000 µM) were assessed. Bacterial cultures were set up in the presence of L-rhamnose, and expression was induced with 400 µM IPTG, added in the late exponential phase of bacterial growth at 37°C for 4 h. Expression was analyzed by SDS-PAGE, both the soluble and insoluble fraction (Fig. 2). No specific protein band was observed at the expected size in the soluble fraction (Fig. 2A), but in the insoluble fraction an intense protein band migrating at the expected size for LAPLm (~62 kDa) at 400 µM IPTG and 0 µM L-rhamnose was observed (Fig. 2B). This band is absent in the lanes corresponding to increasing L-rhamnose concentrations, as well as in uninduced strain transformed with the genetic construct and not supplemented with L-rhamnose (this last condition, in both soluble and insoluble fractions) (Fig. 2A and B).
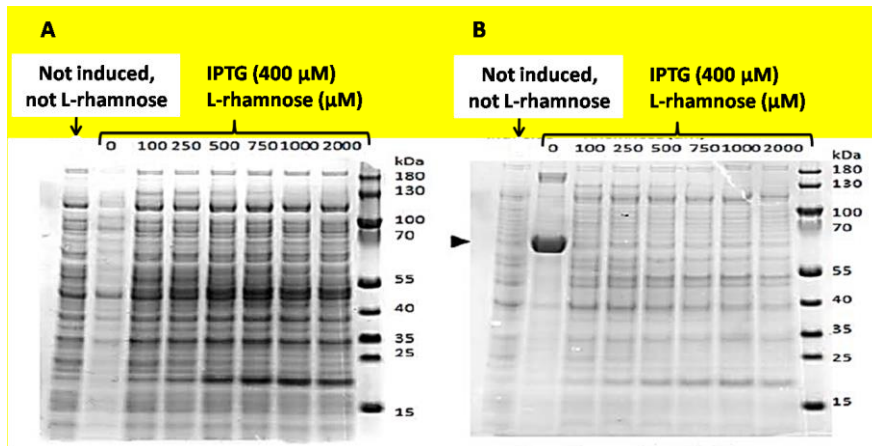
Fig. 2. Small-scale expression of the *laplm* gene in *E. coli* Lemo21(DE3). A) Soluble fraction. B) Insoluble fraction. Expression was induced with 400 μM IPTG in late exponential phase at 37ºC for 4 h. LAPLm is signaled by an arrow.

Lower L-rhamnose concentrations were assessed (1, 20 and 50 μM), inducing the expression with 400 μM IPTG in the late exponential phase of the bacterial growth, overnight at 30ºC. Again, the recombinant protein was not observed in the soluble fraction at none of the L-rhamnose concentrations assayed, and in uninduced strain transformed with the genetic construct and not supplemented with L-rhamnose (Fig. 3). However, a protein with the size expected for LAPLm was observed in the insoluble fraction, at higher concentration when the L-rhamnose concentration diminished.
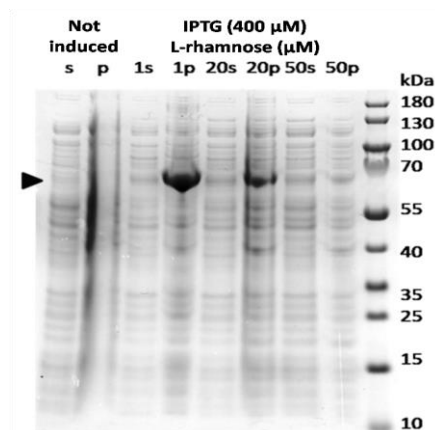

Fig. 3. Small-scale expression of the *laplm* gene in *E. coli* Lemo21(DE3) at lower L-rhamnose concentrations. Expression was induced with 400 μM IPTG in late exponential phase overnight at 30ºC. 1, 20 and 50: 1, 20 and 50 μM L-rhamnose. s: soluble fraction, p: insoluble fraction (pellet). LAPLm is signaled by an arrow.

To further corroborate the presence of the recombinant protein in the soluble fraction, we performed a western-blotting analysis using this fraction and probing against the histidine tag. Using this approach, the protein of interest was detected at all L-rhamnose concentrations tested, but was absent in the negative controls (Fig. 4). This indicates that, in the presence of L-rhamnose, LAPLm is expressed in soluble form, although at yields that are lower than the detection limit of the chromogenic techniques used here. Nevertheless, we assumed that the soluble enzyme is properly folded and therefore should be active when compared to the insoluble protein. Therefore, we decided to focus on the soluble fraction for further purification and kinetic studies.
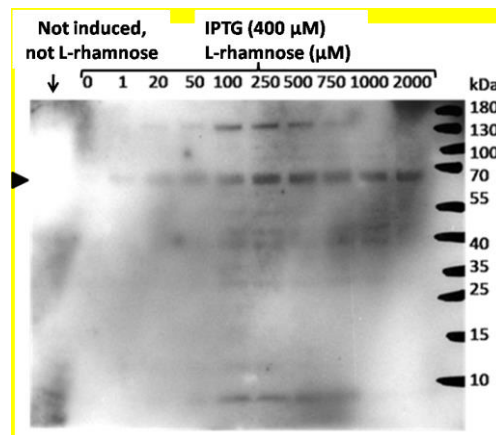

Fig. 4. Western-blot with an anti-His antibody performed with the soluble fractions from the small-scale expression experiments. The expression was performed in *E. coli* Lemo21(DE3) by induction with 400 μM IPTG in late exponential phase at 37ºC for 4 h (uninduced, 0, 100-2000 μM L-rhamnose) or overnight at 30ºC (1, 20 and 50 μM L-rhamnose). LAPLm is signaled by an arrow.

The rLAPLm gene expression was also evaluated by determination of aminopeptidase EA toward the Leu-*p*NA substrate in the cell-free soluble protein extract. Aminopeptidase activity was detected in the extracts of the induced cultures of *E. coli* Lemo21(DE3)/pET-15b-LAPLm, treated with L-rhamnose, and was absent in the extracts of the negative controls. This EA was sensitive to bestatin, the generic inhibitor of the M17 family aminopeptidases, confirming the production of active and soluble rLAPLm in *E. coli* Lemo21(DE3) (data not shown).

3.3. Purification of the rLAPLm enzyme by immobilized metal ion affinity chromatography

To perform the purification of the recombinant protein, rLAPLm was expressed at 300-mL-scale (four cultures), inducing with 400 µM IPTG in late exponential phase of the bacterial growth overnight at 30ºC, and adding 250 µM L-rhamnose (the selected concentration) at the beginning of the culture. The biomass was broken by sonication and insoluble material removed by centrifugation.

The purification of the rLAPLm enzyme in a single step was performed by IMAC using a commercial resin that contains Co^{2+} as immobilized divalent metal cation that specifically interacts with the His-tag of the recombinant enzyme. A representative chromatographic profile is shown in Fig. 5A. rLAPLm was eluted by applying a linear gradient of 20-400 mM imidazole.
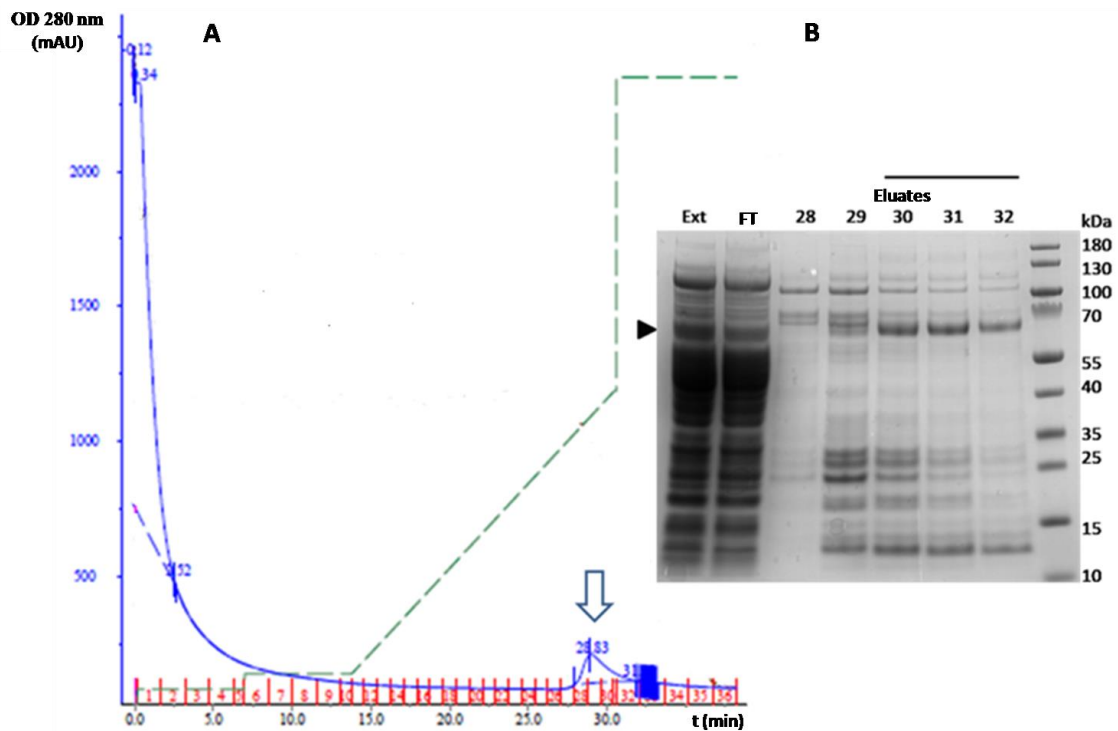

Fig. 5. Purification of the rLAPLm enzyme by IMAC from the *Escherichia coli* Lemo21(DE3)/pET-15b-rLAPLm soluble extract enriched in the recombinant protein. A) Representative chromatographic profile IMAC. mAU: milliunits of absorbance. Continuous line: Optical density at 280 nm. Discontinuous line: imidazole concentration. Numbers above abscise axis: fractions. Eluate is indicated by an arrow. B) Evaluation by SDS-PAGE (NuPAGE 4-12 % Bis-Tris Gel, Coomasie staining). Ext: extract. FT: flow-through. Selected eluates are signaled by a bar. LAPLm is signaled by an arrow.

The results of the purification approach revealed an increase in the intensity of the ~62 kDa protein band in the eluted fractions. Importantly, the IMAC approach effectively concentrates the recombinant protein and this is therefore detectable using Coomassie blue (Fig. 5B). In addition, other proteins co-eluted with the soluble recombinant protein and therefore indicate that these fractions are not homogeneous for rLAPLm. It is unclear whether these additional bands are degradation products or contaminants that bind to the recombinant protein with high affinity. Densitometric analysis of the Coomassie stained SDS-PAGE gel indicated a volumetric yield of 2.5 mg of the purified recombinant enzyme per L of culture.

The three final eluates of each run were pooled and subjected to a gel filtration chromatography in desalting mode, with the aim to eliminate imidazole, which interferes with the metalo-aminopeptidases EA assays. It was confirmed that the purified enzyme has aminopeptidase activity. A summary of the purification process is presented in Table 1. rLAPLm was obtained in a single step from the extract, with a yield of 11 % and a purification factor of 26 times.

Table 1. Summary of the purification process of the rLAPLm enzyme

Purification step	EA (U)	Yield (%)	specEA (U/mg)	PF (times)
Extract	666.7 ± 75.0	100	0.021 ± 0.002	1
IMAC + desalting	75.2 ± 6.8	11	0.54 ± 0.03	26

EA: enzymatic activity. The aminopeptidase activity was assessed toward 300 μM Leu-pNA substrate. U: units. The EA unit is defined as the amount of enzyme necessary to hydrolyze 1 μmol substrate per minute under assay conditions. specEA: Specific enzymatic activity. PF: purification factor. IMAC: immobilized metal ion affinity chromatography. Means ± standard deviations of four replicates are shown.

3.4. Kinetic characterization of the rLAPLm enzyme

We next focused on characterizing multiple kinetic parameters on the purified rLAPLm, including optimal pH, substrate specificity, temperature, and metallic cofactors that might be required for optimal activity.

3.4.1. Effect of pH on rLAPLm aminopeptidase activity

First, the effect of pH on rLAPLm aminopeptidase activity, toward the Leu-pNA substrate, was studied. The maximum activity was registered at pH 7.0, with an abrupt fall of activity at pH 6.0 and 8.0 (around 20 % of maximum activity; Fig. 6). In the rest of the basic zone, the values remained between 11 and 20 % of the maximum activity.

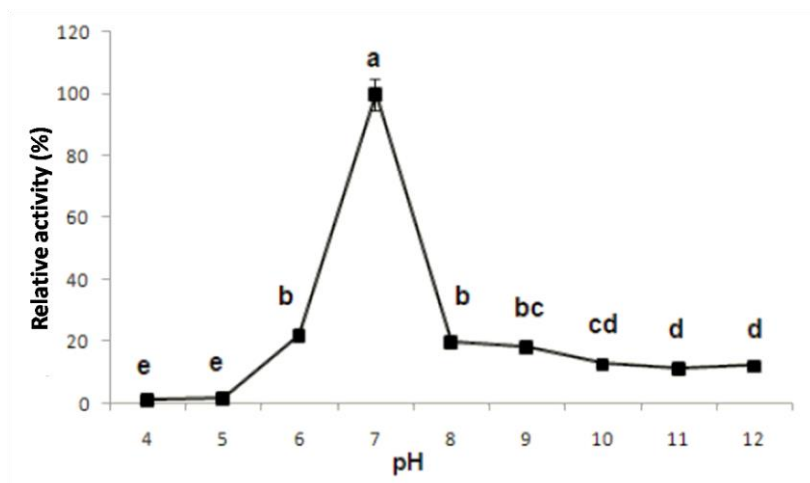However, in the acid zone (pH 4.0-5.0), the relative activity fell below 10 % of the activity at pH 7.0.

Fig. 6. Effect of pH on rLAPLm aminopeptidase activity. The assays were performed with 300 μM Leu-*p*NA substrate and an enzyme concentration of 1.39×10^{-8} M. The activity was normalized using the highest activity as 100 % (corresponding to pH 7.0). The values are represented as the means ± the standard deviations (n = 4). The means were compared by the Tukey HSD test [32], using the software STATISTICA v8.0.550. Different letters represent significant differences for $p < 0.05$.

3.4.2. Substrate specificity of the rLAPLm enzyme

Next, the substrate specificity of rLAPLm enzyme was studied. For this, aminoacyl-*p*NA substrates with different physico-chemical properties of their side chains were tested. As expected, the highest value of EA was obtained with Leu-*p*NA (Fig. 7). In the second position, with 74 % relative activity, Arg-pNA was placed. For the rest of the amino acids evaluated in the substrate P1 position, activity values were lesser than 50 %, regarding the activity registered for Leu-*p*NA.
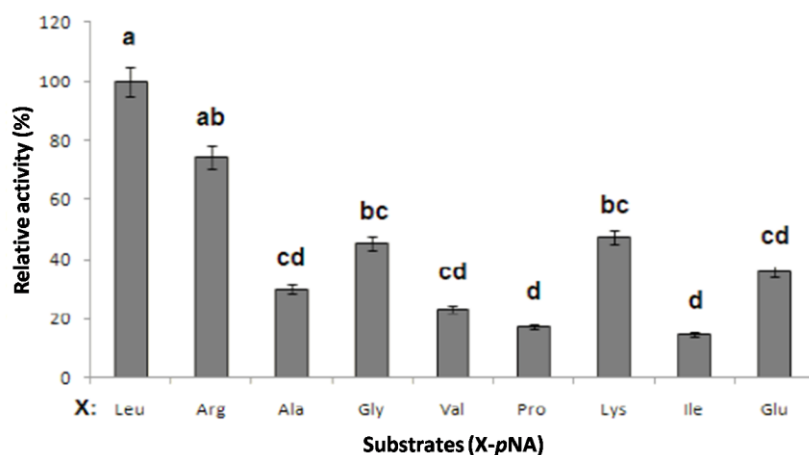
Fig. 7. Substrate specificity of the rLAPLm enzyme. The assays were performed with 300 μM aminoacyl-pNA substrates and an enzyme concentration of 1.39×10^{-8} M. The activity was normalized against the highest activity (corresponding to the Leu-pNA). The values are represented as the means ± the standard deviations (n = 4). The means were compared by the Tukey HSD test [32], using the software STATISTICA v8.0.550. Different letters represent significant differences for p < 0.05.

3.4.3. Kinetic parameters of the rLAPLm enzyme toward the Leu-pNA substrate

Next, the kinetic parameters of the recombinant aminopeptidase toward the Leu-pNA substrate were determined. As rLAPLm was not purified until full homogeneity (Fig. 5B), the kinetic parameters determined in this work are expressed as apparent values. A Michaelis-Menten curve obtained for this enzyme is shown in Fig. 8, and Table 2 lists the values of the resultant kinetic parameters (appK_M, appk_{cat} and apparent k_{cat}/K_M (appk_{cat}/K_M)).
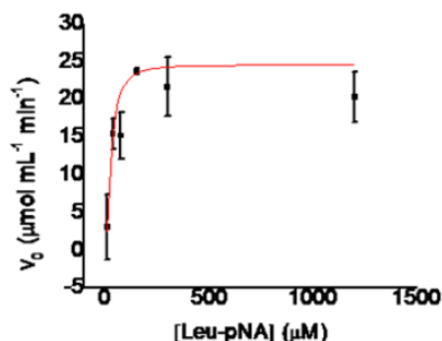

Fig. 8. Effect of substrate concentration on rLAPLm aminopeptidase activity. Six concentrations of the Leu-pNA chromogenic substrate were evaluated covering the range 9.375-1200 μM. The enzyme concentration in the assay was 1.39×10^{-8} M. The function of the Michaelis-Menten's rectangular hyperbola was fitted to the experimental

data, represented as the means ± the standard deviation (n = 4), using the software OriginPro 8 SR0 (version 8.0724 (B724); Origin-Lab Corporation [http://www.OriginLab.com]).

Table 2. Apparent kinetic parameters of the rLAPLm enzyme toward the Leu-*p*NA chromogenic substrate

appK$_M$ (µM)	appk$_{cat}$ (s^{-1})	appk$_{cat}$/K$_M$ (L mol^{-1} s^{-1})
30 ± 8	14.7 ± 1.3	488,483 ± 36,012

The enzyme concentration in the assay was 1.39×10^{-8} M. The values are represented as the means ± the standard error (n = 4).

3.4.4. Effect of temperature on rLAPLm aminopeptidase activity

Subsequently, the effect of temperature on rLAPLm EA was evaluated, testing ten temperature values in the 20-90ºC range (Fig. 9). The enzyme was thermophilic, since the optimum activity was reached at 50ºC. At 30ºC the enzyme retains 70 % of this maximum activity and almost 40 % at 90ºC.
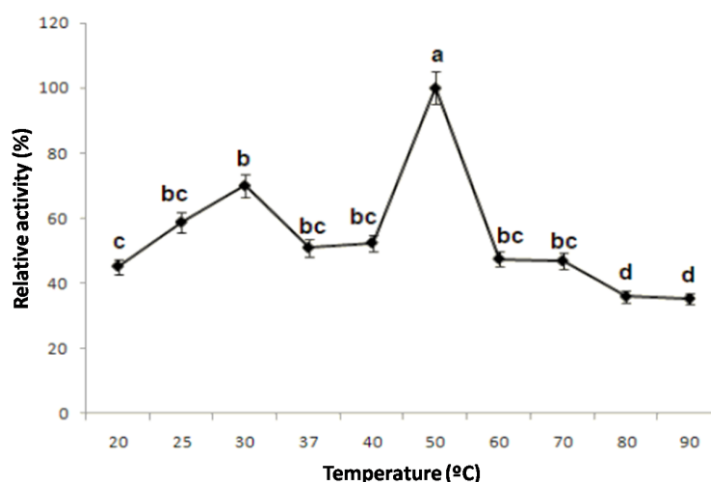

Fig. 9. Effect of temperature on rLAPLm aminopeptidase activity. The assays were performed with 300 µM Leu-*p*NA substrate (~10 appK$_M$) and an enzyme concentration of 1.39×10^{-8} M. The activity was normalized using the highest activity as 100 % (corresponding to 50ºC). The values are represented as the means ± the standard deviations (n = 4). The means were compared by the Tukey HSD test [32], using the software STATISTICA v8.0.550. Different letters represent significant differences for p < 0.05.

3.4.5. Effect of divalent metallic cations on rLAPLm aminopeptidase activity

Additionally, the effect of various divalent metal cations on the rLAPLm EA was studied. These ions function as enzymatic cofactors in the catalytic mechanism of metalo-aminopeptidases [34]. The aim of this experiment was to determine the most appropriate divalent metal cation to supplement the desalted rLAPLm preparation, in the case of potential metal loss from the active site, for example caused by the presence of imidazole or by exchange with Co^{2+} during IMAC. All ions were tested at 4 mM.

As shown in the Fig. 10, the aminopeptidase activity of the purified recombinant enzyme did not vary significantly in the presence of Co^{2+}, Mg^{2+}, Ca^{2+} or Ba^{2+}. However, it was activated by Zn^{2+} (76 times), Mn^{2+} (326-fold) or Cd^{2+} (246 times). This indicates the need to supplement the enzyme preparation with 4 mM $MnCl_2$ or $CdCl_2$, the main activators, for optimum activity in the tested conditions.
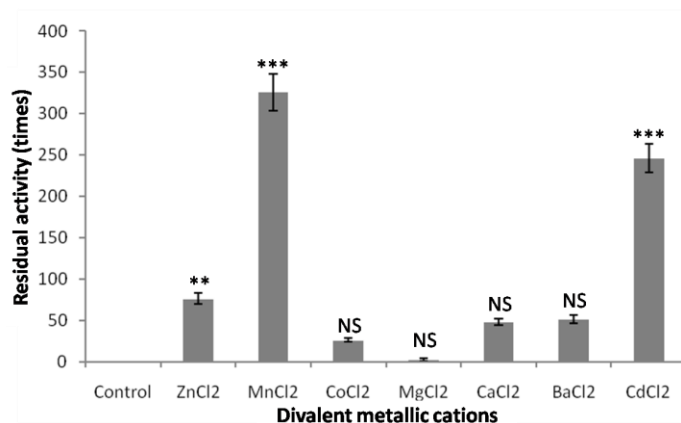

Fig. 10. Effect of divalent metallic cations on rLAPLm aminopeptidase activity. The assays were performed with 30 µM Leu-pNA substrate (~1 appK_M) and an enzyme concentration of 1.39×10^{-8} M. The divalent metallic cations were used in the assay at 4 mM. The residual activity was defined as the quotient between the reaction speed in presence of a given metallic cation and the reaction speed corresponding to the control without cation addition (expressed in times). The values are represented as the means ± the standard deviations (n = 4). The means were compared by the Dunnett test [33], using the software STATISTICA v8.0.550. Two and three asterisks represent significant differences for p < 0.01 and 0.001, respectively. NS: There are not significant differences for p < 0.05.

3.4.6. Inhibition profile for rLAPLm aminopeptidase activity

The inhibition of the rLAPLm aminopeptidase activity toward the Leu-pNA substrate was studied for protease inhibitors of different mechanistic classes. As expected for a M17 LAP, the recombinant enzyme is insensitive to PMSF and TLCK (inhibitors of

serine-proteases), E-64 (inhibitor of cysteine-proteases) and pepstatin A (inhibitor of aspartyl-proteases) (Fig. 11) [35]. In contrast, rLAPLm is inhibited by EDTA (chelating agent for divalent metallic cations; [35]) and bestatin (inhibitor of different metalo-aminopeptidases; [34]).
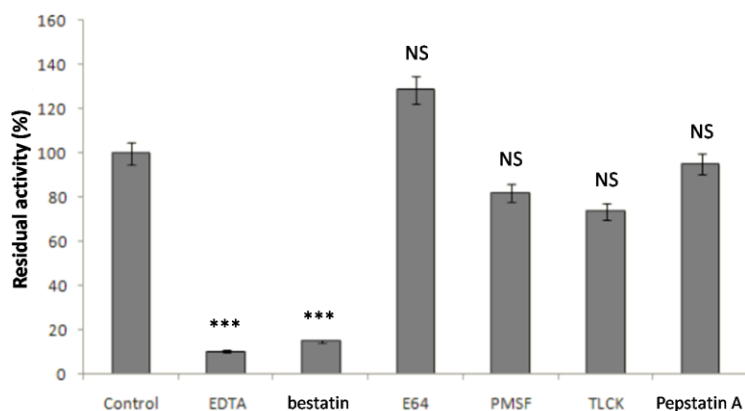

Fig. 11. Inhibition profile for the rLAPLm aminopeptidase activity. The assays were performed with 30 μM Leu-pNA substrate (~1 appK_M) and an enzyme concentration of 1.39×10^{-8} M. The enzyme-inhibitor mixtures were preincubated for 30 min at 25ºC and pH 7.0 before adding the substrate. The controls were prepared by the enzyme preincubation with the same volume of the solvent used to dissolve each inhibitor. The residual activity was defined as the quotient between the reaction velocity in the presence of inhibitor and the reaction velocity of the corresponding control. The values are represented as the means ± the standard deviations (n = 4). The means were compared by the Dunnett test [33], using the software STATISTICA v8.0.550. Three asterisks represent significant differences for p < 0.001. NS: There are not significant differences for p < 0.05.

3.4.7. Partial kinetic characterization of the rLAPLm inhibition by bestatin

Finally, some kinetic characteristics of the rLAPLM inhibition by bestatin were assessed. An IC$_{50}$ value of 14.7 μM for bestatin toward this enzyme and the Leu-pNA substrate was determined (Fig. 12A). On the other hand, bestatin is a non-competitive inhibitor of rLAPLm (Fig. 12B), with an α and a K$_i$ value of 0.7 and 994 nM, respectively (Fig. 12C and D).
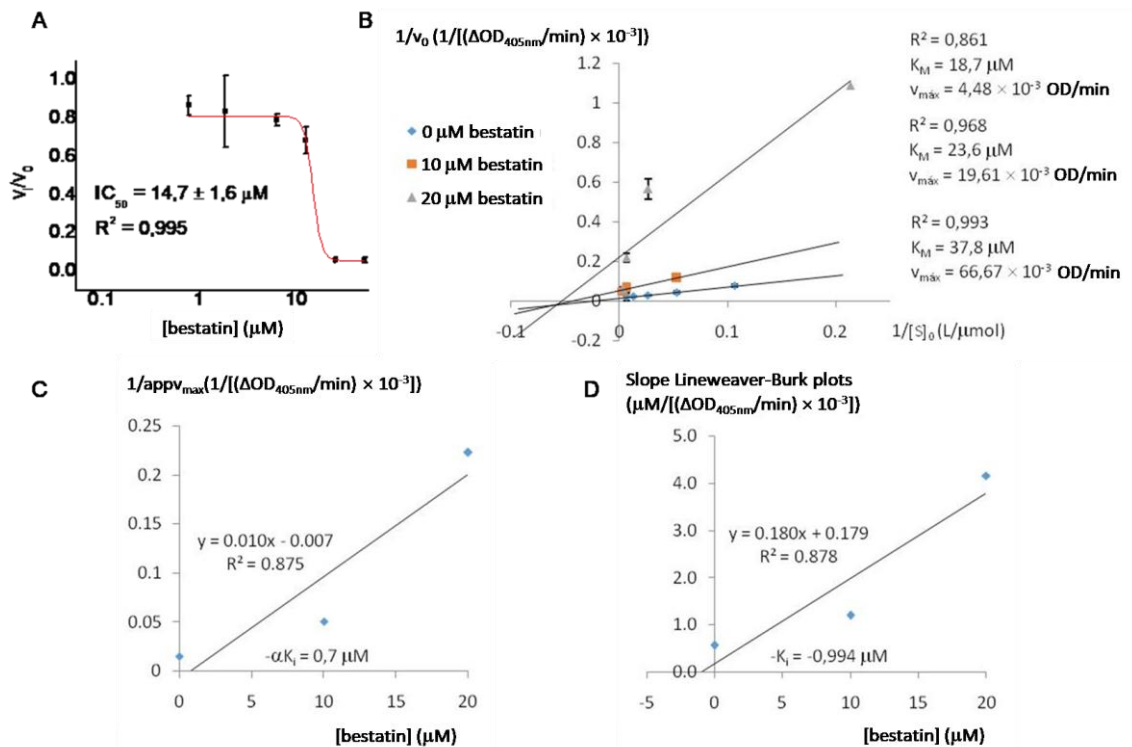
Fig. 12. Some kinetic characteristics of the rLAPLm inhibition by bestatin. In both studies, the assays were performed with an enzyme concentration of 1.39×10^{-8} M. A) Dose-effect study. Leu-pNA substrate was used at 30 µM (~1 appK$_M$), and bestatin was tested at 0.78-50 µM. The IC$_{50}$ value was calculated by the nonlinear fit of the logistic function to the experimental data, using OriginPro 8 SR0 software (version 8.0724 (B724); OriginLab Corporation [http://www.OriginLab.com]). Data are presented as the means ± the standard deviations (n = 4) or the standard error (IC$_{50}$ value). v_i/v_0: residual activity. B) Inhibition type determination. Leu-pNA substrate was used at 4.69-300 µM, and bestatin was tested at 0, 10 and 20 µM. The transformed experimental data (Lineweaver-Burk double reciprocal plots) were analyzed by a simple linear fitting using the software Microsoft Office Excel 2007™ (Microsoft Corporation; USA; [https://www.micro soft.com/]). The inhibition type was determined graphically from the lines of the double reciprocal plots [31]. K$_M$ and v_{max} values are apparent. All data are presented as the means ± the standard deviations (n = 4). C) Dixon plot to determine the -αK$_i$ value (intercept with the abscise axis). D) Secondary plot to determine de -K$_i$ value (intercept with the abscise axis).

4. Discussion

The experimental design for expression of the rLAPLm gene was based on the report of Morty and Morehead [13], who used the gene directly amplified from parasite genomic DNA for expression in *E. coli* BL21(DE3), by induction with 1 mM IPTG for 4 h at 37ºC. The major differences here are the use of a synthetic gene (Fig. 1), codon-optimized and expressed in *E. coli* Lemo21(DE3) by induction with 400 µM IPTG for 4 h at 37ºC or overnight at 30ºC, in the presence of L-rhamnose (Fig. 2-4).

During a gene optimization the adjustment of different parameters is required to obtain high expression levels of a recombinant protein. First, a ==codon adaptation index== (CAI) value as close as possible to 1.0 is desirable. A CAI = 1.0 indicates that the 100 % of the codons match the highest usage frequency in the host. The CAI value of 0.79 for the *rlaplm* gene in *E. coli*, as a result of its sequence optimization, allowed production of rLAPLm at satisfactory levels in the soluble fraction of the bacterial extract (Fig. 4), sufficient to address the enzyme purification (Fig. 5; Table 1) and kinetic characterization (Fig. 6-12; Table 2).

The expression level of rLAPLm gene in the soluble fraction could not be determined by densitometric analysis of the SDS-PAGE gel, due to none protein band was observed on this fraction at none L-rhamnose concentration (Fig. 2A and 4). However, insoluble expression (in inclusion bodies) was evidenced at 0 μM L-rhamnose, condition in which T7 RNA polymerase is totally active (Fig. 2B). In this condition, a reinforced protein band was observed, matching the strength of the used promoter (T7*lac*). Generally, the strong promoters allow reaching concentrations of the recombinant proteins around 10-30 % of the cell total proteins [36].

The insoluble expression of most rLAPLm could be due to the translation speed is higher than folding process rate, leading to the production of missfolded polypeptidic chains that aggregate (among them or with other cellular components) and precipitate. In addition, it should be considered that rLAPLm is a strange protein for the heterologous system *E. coli*, and it could require some glycosylation type for solubility that the bacterium cannot provide. However, in our research group the *T. cruzi* acidic M17 LAP was expressed mainly soluble (representing the 12.53 % of the total *E. coli* proteins) in the BL21(DE3)pLysS strain [37]. Finally, the rLAPLm soluble expression was observed at all tested L-rhamnose concentrations, on a western-blot with an anti-His antibody (Fig. 4). Other antibody-recognized bands could be contaminants, rLAPLm degradation products or even a protein dimer, having an approximate molecular mass of 124 kDa.

In the reference work of Morty and Morehead [13] these authors also express the soluble protein in the BL21(DE3) strain, but they do not analyze the insoluble fraction and do not show an SDS-PAGE gel corresponding to the expression. Therefore, it is not possible to check if the soluble expression level reached by them was enough to see the protein. In this work, the BL21(DE3) strain was also evaluated, but in all tested

induction conditions (1 mM IPTG, 4 h at 37ºC; 0.1-1 mM IPTG, overnight at 37ºC; 1 mM IPTG, overnight at 25ºC; 300 µM IPTG, 4 h at 12ºC) the protein cannot be observed in the soluble fraction and it was detected in the insoluble fraction (data not shown).

The strategy to fuse a tag of six histidines to the rLAPLm amino terminus allowed purifying the protein in a single step by IMAC (Fig. 5). The low yield obtained, of 11 % (Table 1), is probably due to the affectation of the enzymatic activity during the purification process. In this sense, the M17 LAPs have been described as homohexamers in complex equilibrium with other multimeric forms (some inactive) depending on enzyme concentration [38]. Apparently, the LAPLm monomers do not have catalytic activity [13]. However, the obtained volumetric yield, of 2.5 protein mg per L of culture, was enough to perform the kinetic characterization of the recombinant enzyme (Fig. 6-12; Table 2).

The highest rLAPLm activity, toward the Leu-*p*NA substrate, was detected at pH 7.0 (Fig. 6). The higher values of relative activity at basic pH, regarding acid pH, are consistent with those reported for other M17 LAPs, which show the maximum activity at alkaline pHs [13,37,39-42]. The optimum pH for rLAPLm obtained by Morty and Morehead [13] is 8.5, with a high activity still detectable until pH 10.0. In a similar manner to that observed in this work (Fig. 6), activity diminished rapidly under mildly acidic conditions (pH 6.0), although rLAPLm was stable on a wide pH range (pH 4.0-11.0) [13]. In this work, at pH 6.0 and 8.0, the values fell until approximately 20 % of the activity measured at pH 7.0 (Fig. 6). For this reason, we decided to work at pH 7.0 in all aminopeptidase activity assays. The disparities observed between both LAPLm recombinant variants could be due to subtle differences in the folding of both enzymes. As it is known, a recombinant form of an enzyme does not have to be exactly equal to another recombinant form of the same enzyme [43].

The observed maximum aminopeptidase activity toward the Leu-*p*NA substrate, among nine assayed (Fig. 7), confirms the LAP character of this enzyme [13]. Among the other eight aminoacyl-*p*NA substrates evaluated, Arg-*p*NA was the second, with 74 % of activity, compared with Leu-*p*NA. There are data on literature about tomato and porcine LAPs, able to hydrolyze substrates with arginine in P1 position with more than 30 % of relative activity [39]. The acidic M17 LAP from *T. cruzi* also hydrolyzes Arg-*p*NA in the second place of preference, with 55 % of activity regarding Leu-*p*NA [37]. Our

results confirm the narrow substrate specificity of rLAPLm reported by Morty and Morehead [13]. These authors also observed strict aminopeptidase activity against the substrates Cys-, Met-, Ala-, Ile- and Trp-7-amido-4-methylcoumarin (AMC). On the contrary, other M17 LAPs from bacteria, plants and animals show a very broad substrate specificity that includes Leu, Met, Arg, Ala, Ile, Phe, Val, Thr and Tyr, with reduced activity against Gly, Asp, Pro and Trp [44]. It is important to emphasize that we report in this work for the first time the LAPLm aminopeptidase activity toward aminoacyl-pNA substrates.

Removal of the N-terminal polyhistidine tag from a *L. amazonensis* recombinant M17 LAP expressed on *E. coli* did not vary the kinetic characteristics, indicating that it does not interfere with the catalytic activity [13]. For this reason, we did not remove the His-tag to determine the rLAPLm kinetic parameters (Table 2). The appK_M value of 30 μM (Fig. 8; Table 2), is lower than that obtained by Morty and Morehead [13] for the other recombinant variant of this enzyme toward Leu-AMC (167 μM). Our value is in the same magnitude order than that reported for the *T. cruzi* acidic M17 LAP toward Leu-pNA (74 μM; [37]). Strictly, the kinetic parameters determined in this work for rLAPLm cannot be compared with those of the other recombinant form, which were not determined toward aminoacyl-pNA substrates [13]. However, similar values to those obtained here have been reported for other LAPs using Leu-pNA. For example, the K_M value for the potato LAP is 48 μM [41].

The highest aminopeptidase activity, measured at 50ºC (Fig. 9), confirms the thermophilicity of this kind of enzymes [37,38]. It is notable that at 90ºC, rLAPLm still retains almost 40 % of the activity shown at 50ºC (Fig. 9). In this sense, it is comparable with the acidic M17 LAP from *T. cruzi* obtained by Izquierdo *et al*. [37], which exhibits its maximum at 50ºC and 46 % of the maximum activity at 90ºC. In the case of rLAPLm obtained in this work, the decrease in activity at temperatures higher than 50ºC could be related to the loss of the oligomeric structure or not, according to Cadavid-Restrepo *et al*. [38] for the recombinant and native forms of the *T. cruzi* acidic M17 LAP, respectively. Notably, various LAPs of other sources are also thermophilic [39-42].

Among the seven divalent metal cations tested with rLAPLm, Mn^{2+} and Cd^{2+} were activators in the same extent, and Zn^{2+} in a lesser degree, all at 4 mM (Fig. 10). These results partially match the report of Morty and Morehead [13] for the recombinant

variant of the *L. amazonensis* M17 LAP, where the Mn^{2+} cation at 0.5 mM appears as the main enzyme activator, and inhibited above 10 mM. These authors did not test Cd^{2+}, and Zn^{2+} had little effect at 1 mM and potently inhibited at 10 mM. However, Mg^{2+} and Co^{2+}, which did not activate rLAPLm here, in the mentioned work behaved as activators, at micromolar and millimolar concentrations, respectively. In addition, Ca^{2+}, which in this work did not alter the activity, in the report of Morty and Morehead [13] was toxic, inhibiting the enzyme at 1 mM. All these discrepancies could be due to differences between the recombinant protein variants used (rLAPLm in this work and a *L. amazonensis* M17 LAP in the reference work).

In the report of Morty and Morehead [13], the inactive apoenzyme was prepared by incubation with the chelating agent 1,10-phenanthroline and its subsequent removal. Only Mn^{2+} in a greater extent (1 and 5 mM, up to 55 %) and Mg^{2+} in a lesser degree (5 mM, 6-8 %) could reactivate the apoenzyme. As it can be seen, what both studies have in common is the main activating effect of Mn^{2+}. In fact, this is the cation present in the active site of the *T. cruzi* acidic M17 LAP produced in *E. coli*, according to Timm *et al*. [17].

Metalo-aminopeptidases show a wide range of dependence for metal ions. M13 LAPs from mammals typically use Zn^{2+} [45], while other aminopeptidases use Mn^{2+} [46], Fe^{2+} [47] and Zn^{2+} [48]. Regarding Zn^{2+}, the results of Morty and Morehead [13] suggest that this is the natural metal cofactor of LAPLm (at least of the recombinant variant produced in *E. coli*), as was determined by inductively coupled plasma-atomic emission spectrometry (ICP-AES). The Mn^{2+} and Zn^{2+} concentrations are in the range 10-100 μM in the cytosol of trypanosomatid parasites. It is possible that the rLAPLm activation observed in the presence of Mn^{2+} and other metallic cations is due to the ion exchange by the Zn^{2+} from the binding site 1 (which is easily exchanged) [49], while the Zn^{2+} from site 2 (more strongly bound) remains bound [13].

On the other hand, rLAPLm shows an inhibition profile typical of a metalo-aminopeptidase belonging to the M17 family (Fig. 11). The enzyme is inhibited significantly by bestatin and EDTA and is much less sensitive to the inhibition by other protease inhibitors of other mechanistic classes. This result matches the one obtained by Morty and Morehead [13], working with the *L. amazonensis* M17 LAP, and by Cadavid-Restrepo *et al*. [38] and Izquierdo *et al*. [37] working with the native and

recombinant *T. cruzi* acidic M17 LAP, respectively. In addition, it is in agreement with reports by other authors for LAPs from various sources [39,40,42].

The IC_{50} and K_i values (14.7 μM and 994 nM, respectively) determined in this work for bestatin toward rLAPLm (Fig. 12A and D), indicate that this compound is a potent inhibitor of this enzyme, as is expected for an M17 LAP [50,51]. Furthermore, they roughly match the values determined by Izquierdo *et al*. [37] for the *T. cruzi* acidic M17 LAP ($IC_{50} = 6.62$ μM and $K_i = 881$ nM). In another work, an IC_{50} value between 10 and 100 μM (in the same order than in this work; Fig. 12A) for the inhibition of the *Plasmodium vivax* M17 LAP by bestatin is reported [52]. However, Morty and Morehead [13] reported a much lower K_i value (3 nM) for the *L. amazonensis* M17 LAP.

The non-competitive ($\alpha < 1$) inhibition type determined in this work for bestatin toward rLAPLm (Fig. 12B and C) contradicts the generally accepted classification of this pseudopeptide as a competitive inhibitor of many metalo-aminopeptidases [25,34,53]. Such competitive effect of bestatin toward these enzymes is not based in literature on kinetic studies at different substrate and bestatin concentrations, but is based on structural studies. However, generally the 3D structure of these enzymes is determined in the absence of substrate, in which case the inhibitor can be accommodated at the substrate-binding site, as is expected for a competitive inhibitor. It is possible that in the simultaneous presence of substrate and inhibitor, the latter is accommodated in a different site than the substrate affecting the catalytic activity, as is expected for non-competitive or uncompetitive inhibitors [31]. Bestatin is also a non-competitive inhibitor of the *T. cruzi* acidic M17 LAP [37].

Bestatin is well tolerated by experimental animals, with an oral medium lethal dose (LD_{50}) in mice of more than 4 g/kg [54]. Since LAPs from *Leishmania* spp. are responsible for the major LAP activity in these parasites, their selective targeting by inhibitors could interfere with the viability of these microorganisms. Therefore, the presented data may help on this enzyme validation as a novel drug target [55].

5. Conclusions

In summary, rLAPLm is similar to the recombinant enzyme obtained by Morty and Morehead [13] in the following kinetic characteristics: (i) substrate specificity for

leucine at the P1 position; (ii) main activation by Mn^{2+}; (iii) inhibition profile; and (iv) potent inhibition by bestatin. These similarities indicate that rLAPLm can be used as a model of the native enzyme for inhibitors identification.

References

[1]   M.C. Field, D. Horn, A.H. Fairlamb, M.A.J. Ferguson, D.W. Gray, K.D. Read, M. De Rycker, L.S. Torrie, P.G. Wyatt, S. Wyllie, I.H. Gilbert, Anti-trypanosomatid drug discovery: an ongoing challenge and a continuing need, Nature Rev. Microbiol. (2017). doi: 10.1038/nrmicro.2016.193

[2]   H. Hussain, A. Al-Harrasi, A. Al-Rawahi, I.R. Green, S. Gibbons, Fruitful decade for antileishmanial compounds from 2002 to late 2011, Chem. Rev. 114 (2014) 10369-10428.

[3]   World Health Organization, Leishmaniasis fact sheet, World Health Organization, Geneva, Switzerland. http://www.who.int/mediacentre/factsheets/fs375/en/, 2017 (accessed 16 December 2020).

[4]   E. Handman, Leishmaniasis: current status of vaccine development, Clin. Microbiol. Rev. 14 (2001) 229-243.

[5]   S. Sundar, A. Singh, Recent developments and future prospects in the treatment of visceral leishmaniasis, Ther. Adv. Infect. Dis. 3 (2016) 98-109.

[6]   S.Y. Bhat, A. Dey, I.A. Qureshi, Structural and functional highlights of methionine aminopeptidase 2 from *Leishmania donovani*, Int. J. Biol. Macromol. 115 (2018) 940-954.

[7]   S. Mohapatra, Drug resistance in leishmaniasis: newer developments, Trop. Parasitol. 4 (2014) 4. doi: 10.4103/2229-5070.129142

[8]   J.C. Mottram, D.R. Brooks, G.H. Coombs, Roles of cysteine proteinases of trypanosomes and Leishmania in host-parasite interactions, Curr. Opin. Microbiol. 1 (1998) 455-460.

[9]   J. Bouvier, P. Schneider, R. Etges, Leishmanolysin: Surface metalloproteinase of *Leishmania*. Meth. Enzymol. 248 (1995) 614-633.

[10]   R.E. Morty, J.D. Lonsdale-Eccles, J. Moreheadi, E.V. Caleri, R. Mentele, E.A. Auerswald, T.H.T. Coetzer, N.W. Andrewsi, B.A. Burleigh, Oligopeptidase B from *Trypanosoma brucei*, a new member of an emerging subgroup of serine oligopeptidases, J. Biol. Chem. 274 (1999) 26149-26156.

[11]   N.D. Rawlings, A.J. Barrett, P.D. Thomas, X. Huang, A. Bateman, R.D. Finn, The MEROPS database of proteolytic enzymes, their substrates and inhibitors in 2017 and a comparison with peptidases in the PANTHER database, Nucleic Acids Res. 46 (2018) 624-632.

[12]   G. Knowles, The effects of arphamenine-A, an inhibitor of aminopeptidases, on *in-vitro* growth of *Trypanosoma brucei brucei*, J. Antimicrob. Chemother. 32 (1993) 172-174.

[13]   R.E. Morty, J. Morehead, Cloning and characterization of a leucyl aminopeptidase from three pathogenic *Leishmania* species, J. Biol. Chem. 277 (2002) 26057-26065.

[14] M.B. Harbut, G. Velmourougane, S. Dalal, G. Reissa, J.C. Whisstock, O. Onder, D. Brisson, Sh. McGowan, M. Klemba, D.C. Greenbaum, Bestatin-based chemical biology strategy reveals distinct roles for malaria M1- and M17-family aminopeptidases, Proc. Natl. Acad. Sci. USA 108 (2011) E526-534.

[15] R. Kumar, K. Tiwari, V.K. Dubey, Methionine aminopeptidase 2 is a key regulator of apoptotic like cell death in *Leishmania donovani*, Sci. Rep. 7 (2017) 95. doi: 10.1038/s41598-017-00186-9

[16] P. Peña-Díaz, M. Vancová, C. Resl, M.C. Field, J. Lukeš, A leucine aminopeptidase is involved in kinetoplast DNA segregation in *Trypanosoma brucei*, PLoS Pathog. 13 (2017) e1006310. doi: 10.1371/journal.ppat.1006310

[17] J. Timm, M. Valente, D. García-Caballero, K.S. Wilson, D. González-Pacanowska, Structural characterization of acidic M17 leucine aminopeptidases from the TriTryps and evaluation of their role in nutrient starvation in *Trypanosoma brucei*, mSphere 2 (2017) e00226-17. doi: 10.1128/mSphere.00226-17.

[18] M. Matsui, J.H. Fowler, L.L. Walling, Leucine aminopeptidases: diversity in structure and function, Biol. Chem. 387 (2006) 1535-1544.

[19] G.O. Aboge, S. Cao, M.A. Terkawi, T. Masatani, Y. Goo, M. AbouLaila, Y. Nishikawa, I. Igarashi, H. Suzuki, X.A. Xuan, Molecular characterization of *Babesia bovis* M17 leucine aminopeptidase and inhibition of *Babesia* growth by bestatin, J. Parasitol. 101 (2015) 536-541.

[20] Y-R. Lee, B-K. Na, E-K. Moon, S-M. Song, S-Y. Joo, H-H. Kong, Y.K. Goo, D.I. Chung, Y. Hong, Essential role for an M17 leucine aminopeptidase in encystation of *Acanthamoeba castellanii*, PLoS ONE 10 (2015) e0129884. doi: 10.1371/journal.pone.0129884

[21] J. Zheng, H.L. Jia, Y.H. Zheng, Knockout of leucine aminopeptidase in *Toxoplasma gondii* using CRISPR/Cas9, Int. J. Parasitol. 45 (2015) 141-148.

[22] G. Maggioli, G. Rinaldi, I. Giaudrone, P. Berasain, J.F. Tort, P.J. Brindley, C. Carmona, Expression, purification and characterization of two leucine aminopeptidases of the blood fluke, *Schistosoma mansoni*, Mol. Biochem. Parasitol. 219 (2018) 17-23.

[23] G. Curien, V. Biou, C. Mas-Droux, M. Robert-Genthon, J.L. Ferrer, R. Dumas, Amino acid biosynthesis: New architectures in allosteric enzymes, Plant Physiol. Biochem. 46 (2008) 325-339.

[24] M. Izquierdo, D. Lin, S. O'Neill, M. Zoltner, L. Webster, A. Hope, D.W. Gray, M.C. Field, J. González-Bacerio, Development of a high-throughput screening assay to identify inhibitors of the major M17-leucyl aminopeptidase from *Trypanosoma cruzi* using RapidFire mass spectrometry, SLAS Discovery (2020). doi: 10.1177/2472555220923367.

[25] H. Umezawa, T. Aoyagi, H. Suda, M. Hamada, T. Takeuchi, Bestatin, an inhibitor of aminopeptidase B, produced by actinomycetes, J. Antibiot. (Tokyo) 29 (1976) 97-99.

[26] A. Trochine, D.J. Creek, P. Faral-Tello, M.P. Barrett, C. Robello, Bestatin induces specific changes in *Trypanosoma cruzi* dipeptide pool, Antimicrob. Agents Chemother. 59 (2015) 2921-2925.

[27] U.K. Laemmli, Cleavage of structural proteins during the assembly of the head of bacteriophage T4, Nature 227 (1970) 680-685.

[28] P.K. Smith, R.I. Krohn, G.T. Hermanson, A.K. Mallia, F.H. Gartner, M.D. Provenzano, E.K. Fujimoto, N.M. Goeke, B.J. Olson, D.C. Klenk, Measurement of protein using bicinchoninic acid, Anal. Biochem. 150 (1985) 76-85.

[29] S. Tieku, N.M. Hooper, Inhibition of aminopeptidases N, A and W: A re-evaluation of and inhibitors of angiotensin converting enzyme, Biochem. Pharmacol. 44 (1992) 1725-1730.

[30] J.W. London, L.M. Shaw, D. Fetterolf, D. Garfinkel, Determination of the mechanism and kinetic constants for hog kidney γ-glutamyltransferase, Biochem. J. 157 (1976) 609-617.

[31] R.A. Copeland, Enzymes: A practical introduction to structure, mechanism, and data analysis, second ed., Wiley-VCH, Inc., Nueva York, 2000.

[32] J. Tukey, Comparing individual means in the analysis of variance, Biometrics 5 (1949) 99-114.

[33] C.W. Dunnett, New tables for multiple comparisons with a control, Biometrics 20 (1964) 482-491.

[34] A. Mucha, M. Drag, J.P. Dalton, P. Kafarski, Metallo-aminopeptidase inhibitors, Biochimie 92 (2010) 1509-1529.

[35] Sigma Life Science, Protease inhibition and detection, Life Science BioFiles 4 (2009) 1-30.

[36] S.C. Makrides, Strategies for achieving high-level expression of genes in *Escherichia coli*, Microbiol. Reviews. 60 (1996) 512-538.

[37] M. Izquierdo, M.E. Aguado, M. Zoltner, J. González-Bacerio, High-level expression in *Escherichia coli*, purification and kinetic characterization of LAPTc, a *Trypanosoma cruzi* M17-aminopeptidase, Protein J. 38 (2019) 167-180.

[38] G. Cadavid-Restrepo, T.S. Gastardelo, E. Faudry, H. de Almeida, I.M. Bastos, R.S. Negreiros, M.M. Lima, T.C. Assumpção, K.C. Almeida, M. Ragno, C. Ebel, B.M. Ribeiro, C.R. Felix, J.M. Santana, The major leucyl aminopeptidase of *Trypanosoma cruzi* (LAPTc) assembles into a homohexamer and belongs to the M17 family of metallopeptidases, BMC Biochem. 12 (2011) 46. doi: 10.1186/1471-2091-12-46

[39] Y-Q. Gu, F.M. Holzer, L.L. Walling, Over expression, purification and biochemical characterization of the wound-induced leucine aminopeptidase of tomato, Eur. J. Biochem. 263 (1999) 726-735.

[40] V. Nagy, K.M. Nampoothiri, A. Pandey, R. Rahulan, G. Sza, Production of L-leucine aminopeptidase by selected *Streptomyce*s isolates, J. Appl. Microb. 104 (2008) 380-387.

[41] Z. Vujčić, B. Dojnov, M. lovanović, N. Božić, Purification and properties of the major leucil aminopeptidase from *Solanum tuberosum* tubers, Fruit Veget. Cereal Sci. Biotechnol. 2 (2008) 125-130.

[42] A.F. Correa, I.M. Bastos, D. Neves, A. Kipnis, A.P. Junqueira-Kipnis, J.M. de Santana, The activity of a hexameric M17 metallo-aminopeptidase is associated with survival of *Mycobacterium tuberculosis*, Front. Microbiol. 8 (2017) 504. doi: 10.3389/fmicb.2017.00504

[43] J. González-Bacerio, A.K. Carmona, M.L. Gazarini, M. Chávez, M. Alonso del Rivero, Kinetic characterization of recombinant PfAM1, a M1-aminopeptidase from *Plasmodium falciparum* (Aconoidaside: Plasmodiidae), using fluorogenic peptide substrates, Rev. Cub. Cienc. Biol. 4 (2015) 40-48.

[44] Y-Q. Gu, L.L. Walling, Specificity of the wound- induced leucine aminopeptidase (LAP- A) of tomato, Eur. J. Biochem. 267 (2000) 1178-1187.

[45] F.H. Carpenter, J.M. Vahl, Leucine aminopeptidase (Bovine lens) mechanism of activation by Mg^{2+} and Mn^{2+} of the zinc metalloenzyme, amino acid composition, and sulfhydryl content, J. Biol. Chem. 248 (1973) 294-304.

[46] G.S. Cottrell, N.M. Hooper, A.J. Turner, Cloning, expression, and characterization of human cytosolic aminopeptidase P: A single manganese(II)-dependent enzyme, Biochemistry 39 (2000) 15121-15128.

[47] V. M. D'Souza, R.C. Holz, The methionyl aminopeptidase from *Escherichia coli* can function as an iron(II) enzyme, Biochemistry 38 (1999) 11079-11085.

[48] K.W. Walker, R.A. Bradshaw, Yeast methionine aminopeptidase I can utilize either Zn^{2+} or Co^{2+} as a cofactor: a case of mistaken identity?, Protein Sci. 7 (1998) 2684-2687.

[49] H.E. van Wart, S.H. Lin, Metal binding stoichiometry and mechanism of metal ion modulation of the activity of porcine kidney leucine aminopeptidase, Biochemistry 20 (1981) 5682-5689.

[50] T.S. Skinner-Adams, J. Lowther, F. Teuscher, C.M. Stack, J. Grembecka, A. Mucha, P. Kafarski, K.R. Trenholme, J.P. Dalton, D.L. Gardiner, Identification of phosphinate dipeptide analog inhibitors directed against the *Plasmodium falciparum* M17 leucine aminopeptidase as lead antimalarial compounds, J. Med. Chem. 50 (2007) 6024-6031.

[51] C.M. Stack, J. Lowther, E. Cunningham, S. Donnelly, D.L. Gardiner, K.R. Trenholme, T.S. Skinner-Adams, F. Teuscher, J. Grembecka, A. Mucha, P. Kafarski, L. Lua, A. Bell, J.P. Dalton, Characterization of the *Plasmodium falciparum* M17 leucyl aminopeptidase. A protease involved in amino acid regulation with potential for antimalarial drug development, J. Biol. Chem. 282 (2007) 2069-2080.

[52] J-Y. Lee, S-M. Song, J-W. Seok, B.K. Jha, E-T. Han, H-O. Song, H-S. Yu, Y. Hong, H-H. Kong, D-I. Chung, M17 leucine aminopeptidase of the human malaria parasite *Plasmodium vivax*, Mol. Biochem. Parasitol. 170 (2010) 45-48.

[53] O.A. Scornik, V. Botbol, Bestatin as an experimental tool in mammals, Curr. Drug. Metab. 2 (2001) 67-85.

[54] T. Sakakibara, K. Ito, Y. Irie, T. Hagiwara, Y. Sakai, M. Hayashi, H. Kishi, M. Sakamoto, M. Suzuki, Y. Irie, Toxicological studies on bestatin. 1. Acute toxicity test in mice, rats and dogs, Jpn. J. Antibiot. 36 (1983) 2971-2984.

[55] A. Vermelho, G. Salvatore, C. d'Avila-Levy, A. Souza do Santos, A.C. Nogueira de Melo, F. Paes Silva, E. da Silva Bom, M.H. Branquinha, Trypanosomatidae peptidases: A target for drugs development, Curr. Enz. Inhib. 3 (2007) 19-48.